Indian Journal of Biochemistry & Biophysics
Vol. 58, June 2021, pp. 292-302

Encapsulation of purple sweet potato's anthocyanin in CMC-PVA matrix for development of paper strips as a colorimetric biosensor

Anting Wulandari[1], Titi Candra Sunarti[1]*, Farah Fahma[1], Erliza Noor[1] & Toshiharu Enomae[2]

[1]Department of Agroindustrial Technology, Bogor Agricultural University, Bogor-16002, Indonesia

[2]Faculty of Life and Environmental Sciences, University of Tsukuba, Ibaraki, 305-8577, Japan

Received 03 October 2019; *revised 31 July 2020*

Bioactive compound from local resources such as anthocyanin has a high potential to develop as a biosensor for nitrite detection. As a biosensor, this compound shows instability to certain environmental conditions. To overcome this, bioactive compound may need to encapsulate. The aim of this work is to encapsulate of anthocyanin in the CMC-PVA matrix to improve its stability as paper strip for sodium nitrite detection. The result of this work shows that anthocyanin encapsulated by CMC/PVA matrix has well formed. Encapsulated anthocyanin has good homogeneity and it was strongly immobilized in the CMC/PVA matrix. Encapsulated anthocyanin is attached to the surface of the paper medium and penetrated into the matrix. The strip is shown changing color from red to yellow as it applied to nitrite. The selectivity of biosensor paper strip system is observed for various other chemicals including heavy metals such as Pb^{2+}, Zn^{2+}, Fe^{3+}, Mg^{2+}, NaCl, boric acid, monosodium glutamate, sodium benzoate, and formalin with a concentration of 10000 ppm, respectively, and the biosensor was selective towards nitrite. This work gives a basic information to development of a practical green sensor in the form of paper strips for nitrite detection with good stability and selectivity.

Keywords: Bioactive compound, Color change, Detection, Nitrite

The diversity of plant resources in Indonesia is a good source for dye and bioactive compounds which will offer the opportunity to become biosensors with unique specificity and sensitivity. Bioactive compound from local resource such as anthocyanin is natural compound that produce color with certain specificity. Anthocyanin was extracted from purple sweet potato (*Ipomoea batatas* L). The typical color of each bioactive can provide different response towards environmental condition and certain chemicals. Based on our previous work, anthocyanin is potentially developed as biosensors for nitrite detection[1]. Anthocyanin is a bioactive component of the flavonoid group that can give red, purple, blue, to flowers, leaves, tubers, fruits and vegetables[2]. The use of anthocyanin as a sensor also has been carried out by previous researchers as pH and borate sensing[3]. In general, the use of bioactive components such as anthocyanin as a biosensor indicator has advantages such as non-toxic, easily renewed, and easy handling. Colorimetric biosensor development in the form of paper has several advantages including cost savings, simplicity, and no requirement of any expensive instruments[4]. However, as biosensor indicator, anthocyanin has poor stability because it is easy to be affected by the environment such as oxygen, light, temperature, and pH, so it is necessary to protect it in a matrix.

In this study, the matrix gel system is a mixture of carboxymethyl cellulose (CMC) and-polyvinyl alcohol (PVA), which has been chosen to maintain the stability of purple sweet potato anthocyanin. CMC is a cellulose derivative obtained through its carboxymethylation. CMC is often used because it has high viscosity, and strong hydrophilicity. CMC hydrogel has a good biodegradability, and low toxicity[5]. PVA as a synthetic polymer, is biodegradable, nontoxic, biocompatible, and water soluble, with high hydrophilicity, good film forming ability and processability[6]. The addition of PVA can increase thermal stability, chemical properties, and water absorption[7]. The objective of this study was to encapsulate of anthocyanin in the CMC-PVA matrix to improve its stability in the development as paper strip for nitrite detection.

*Correspondence:
E-mail: titi-cs@apps.ipb.ac.id

Materials and Methods

Materials

Purple sweet potato *Ayamurasaki*variety was obtained from the local market in Cikarawang, Bogor, Indonesia. Paper strip was developed by using Whatman No.1 filter paper. Matrix for encapsulating the anthocyanin werecarboxymethyl cellulose (CMC) (high viscosity, HiMedia, India), polyvinyl alcohol (PVA), citric acid (Merck) and used as pro analysis grade. Chemicals used were sodium nitrite (Merck), zinc sulfate (Merck), lead (II) nitrate (Merck), ammonium iron (III) sulfate (Merck), magnesium sulfate (Merck), zinc sulfate (Merck), boric acid (Merck), food-grade sodium chloride (NaCl) and monosodium glutamate (MSG), sodium benzoate, and formalin.

Preparation of anthocyanin extract

Purple sweet potato (PSP) was peeled, washed, and sliced of ± 3 mm. Then, it was blanched in hot water for 7 min and then frozen for 24 h. Furthermore it was crushed and blended with the mixture of 96% ethanol, aquadest, and acetic acid (25: 5: 1 (*v/v*)). Anthocyanin slurry was filtered with muslin cloth, and the filtrate was re-filtered with filter paper Whatman No. 41 by using a vacuum filter. The filtrate obtained was centrifuged (IEC Clinical Centrifuge, USA) at 3000 rpm for 15 min. Soluble ethanol was evaporated at 50°C in the water bath, and then anthocyanin extract was stored in the refrigerator before use[8].

Stability of extract anthocyanin to temperature

A total of 5 mL of anthocyanin extract that had been diluted 25 times or its concentration of 11.59 mg/L (1.16×10^{-3} %) was put in a test tube then heated in a water bath at 30, 40, 50, 60, 70, and 80°C for 4 h. Every 1 h, the color intensity was observed with a UV-Vis spectrophotometer at 540 nm. This method refers to Wang *et al.*[9] with modification.

Purity of reagent

In this research, the reagent used as an indicator of nitrite detection is anthocyanin extract without the addition of other chemicals. The anthocyanin extract used was crude ethanol extract with an ethanol content of 50% (not completely evaporated) where the crude extract concentration produced was 289.73 mg/L and used as a reagent in a mixture of CMC/PVA-citric acid solution was 57.95 mg/L or 5.80×10^{-3}%. Where, CMC, PVA and citric acid solutions used were pro grade analysis.

Preparation anthocyanin encapsulation in the CMC/PVAmatrix and its interaction with nitrite

The encapsulation method refers to Zhai *et al*.[10], Shivakumara *et al*.[11] with a slight modification. About 0.75 g of CMC was dissolved in 30 mL of aquadest by continuous stirring at 1200 rpm, temperature 50°C for 6 h until completely dissolved. Then 3 mL of 1% PVA was added to CMC solution. Same volume of 10% citric acid as cross-linking agent was added to the mixture of CMC and PVA solutions. After completely dissolved, 3 mL of anthocyanin extract (57.95 mg/L) was added into the mixture of CMC-PVA-citric acid solution. Finally, the encapsulated anthocyanin was homogenized with UH-600S Ultrasonic Homogenizer. Finally, the anthocyanin gel solution was poured in the petri dish and dried at 50°C for 24 h to get an anthocyanin film. Particle size distribution of encapsulated anthocyanin was measured by zetasizer (Malvern). Thermal properties of encapsulated anthocyanin film was determined using Thermogravimetric Analysis (TGA) at temperature 30-650°C with temperature rise was 10°C/min. Then, interaction between encapsulated anthocyanin and 1% (1000 mg/L) of nitrite solution was analyzed. Microstructure of encapsulated anthocyanins gel and its application for sensing of nitrite were analyzed using Transmission Electron Microscopy (TEM) (Hitachi, H-7650). Study of the functional groups of encapsulated anthocyanin film andits mixture with nitrite were performed using Fourier-Transform Infrared Spectroscopy (FTIR).

Preparation of anthocyanin paper strip for nitrite detection

Preparation of anthocyanin paper strips refers to Anggriawan *et al*.[12] and Wang *et al*.[13] with modification. One piece of filter paper (Whatman No.1) was placed in a petri dish. Subsequently, anthocyanin gel solution was dropped on the surface of paper filter. Afterwards, it was dried in drying oven at 50°C for 24 h. The anthocyanin paper was cut into 1.5 cm × 1.5 cm strips, and then were kept in vacuum plastic bag at room temperature. Furthermore, anthocyanin paper strip was applied for nitrite detection. It was dripped with 1% (10000 mg/kg) nitrite solution as much as 0.2 mL. Absorption of the color into the paper strip was observed using a light microscope (CH10MOMF Olympus). Attachment of encapsulated anthocyanin and its application for sensing of nitrite on paper surface were observed by Scanning Electron Microscope (SEM).

Selectivity of Anthocyanin Paper Strip and the Interferences of the Chemicals

The anthocyanin paper strip was dripped with 10000 ppm chemicals as much as 0.2 mL to examine its selectivity. The chemicals were such as Pb^{2+}, Zn^{2+}, Fe^{3+}, Mg^{2+}, NaCl, boric acid, monosodium glutamate, sodium benzoate, and formalin. In order to investigate the interference of nitrite sensing, in this work 0.2 mL of each chemical was dripped in the anthocyanin paper strip and then followed by 0.2 mL of 1% nitrite. This method refers to Raj & Dhesingh[14] with modification. Color changes in selectivity and interference study tests were measured by using colorimeters following the CIELAB system (L^*, a^*, b^*, c^*, ^{o}Hue, ΔE^*) where L^* indicates brightness (0 = black, 100 = white), a^* [(Greenness (−) to reddish (+)], b^* [(blueness (−) to yellowness (+)]. The color of sample was calculated as the °Hue value, °Hue = $\tan^{-1} b^*/a^*$ (0° or 360° = red, 90° = yellow, 180° = green, and 270° = blue), while saturation of color was calculated from Chroma value (c^*), $c^* = (a^{*2} + b^{*2})^{½}$. ΔE^* indicates the color differences and calculated as $\Delta E^* = ((L_{ti}^* - L_{t0}^*)^2 + (a_{ti}^* - a_{t0}^*)^2 + (b_{ti}^* - b_{t0}^*))^{1/2}$; while L_{ti}^*, a_{ti}^*, b_{ti}^* are the color coordinates after treatment, and before treatment/control (t_0)[15,16]. The morphology of the anthocyanin paper strip in nitrite detection was observed by Scanning Electron Microscope (SEM) and absorption of the color into the paper strip was observed using a light microscope (CH10MOMF Olympus).

Statistical analysis

Statistical analysis of the effect of chemicals and targeted chemical concentrations on paper strip color changes with the CIELAB system (L^*, a^*, b^*, c^*, ^{o}Hue, ΔE^*) was determined by completely randomized trial design with one factor and the data was analysed using IBM SPSS version 22 where the significance of the differences in inter-treatments were tested with the Tukey method ($\alpha = 0.05$).

Results and Discussion

Stability of Anthocyanin Extract to Temperature

Temperature plays an important role in the drying process in making biosensor paper strips. Bioactive compounds are natural compounds that are easily damaged at certain temperatures. To find out the damage of anthocyanin as a bioactive compound that would be developed into a biosensor. In this study, thermal stability analysis was carried out at 30-80°C at various lengths of heating time, 0-4 h. The results showed that anthocyanin decreased absorbance along with the increase of temperatures. Figure 1 exhibits anthocyanin absorbance decreases with time at several temperatures. There was a decrease of absorbance, which started from 40-80°C. Whereas, at 30°C from 0-4 h, the decrease of absorbance was slightly, even tends to be stable. While at 40-80°C the absorbance was increasing over time. The highest decrease of absorbance occurred at 80°C for 4 h which was 26.34% (stability of 73.66%). Thus, anthocyanin color intensity was decreased at high temperatures.

Kinetics degradation of anthocyanin is observed based on reaction rate constants (k) and half-life ($t_{1/2}$). In this study, zero, first and second order reaction kinetics modelling was carried out, as show in (Table 1). A degradation rate constant was

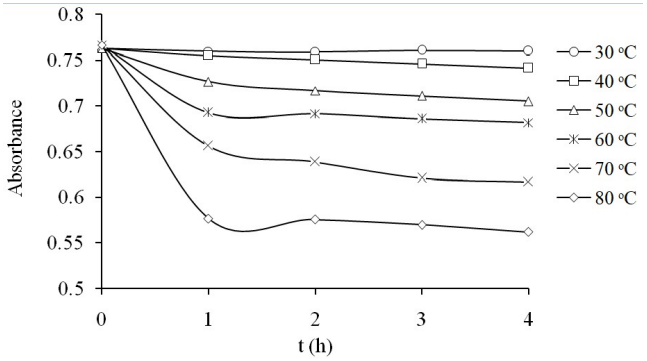

Fig. 1 — Effect of temperature and exposure time to the anthocyanin color intensity at 540

Table 1 — Kinetic parameter of anthocyanin thermal degradation

T (°C)	Pseudo zero order				Pseudo first order				Pseudo second order			
	−k (1/h)	R^2	$t_{1/2}$	Ea (kJ/mol)	−k (1/h)	R^2	$t_{1/2}$	Ea (kJ/mol)	k (1/h)	R^2	$t_{1/2}$	Ea (kJ/mol)
30	0.001	0.177	761		0.0005	0.178	1386.00		0.001	0.177	1876.43	
40	0.007	0.984	59.47		0.007	0.985	99.00		0.009	0.986	141.19	
50	0.016	0.818	23.37		0.018	0.826	38.72		0.025	0.833	54.40	
60	0.023	0.620	16.97	73.39	0.025	0.626	28.26	81.82	0.034	0.611	39.95	90.22
70	0.041	0.736	8.78		0.049	0.755	14.14		0.072	0.775	19.18	
80	0.051	0.564	6.65		0.063	0.574	10.93		0.097	0.585	15.10	

proportional to the temperature rise and inversely to the half-life of the zero order, first order or second order kinetics model. In this study, kinetic degradation dominantly followed by first order kinetics models because it tends to have greater R^2. This is in line with the work of Mulyawanti *et al.*[17]; Jiang *et al.*[18]. In first order kinetics model at 30°C, the k value was 0.012 (1/h). The k value was smaller than those at 40-80°C. The highest k value was at 80°C, which was 0.120 (1/h) in the first order kinetic.

The half-life declined along increased temperature (Table 1). At 30°C, the half-life was 1386.00 h for the first order kinetics model. And the lowest half-life was at 80°C, which was 10.93 h. Anthocyanin purple sweet potato was degraded at 90°C, pH 3 where $t_{1/2}$ was 10.27 h[18]. The structure of anthocyanin from different anthocyanin source, pH, solvent, and anthocyanin concentration possibly affect to the rate of degradation and degradation ratio.

Therefore, based on the results of anthocyanin instability analysis to temperature, then in their development as a biosensor paper strip, they must be encapsulated in a matrix (CMC/PVA matrix) to increase its stability.

Particle size distribution and polydispersity Index

One important parameter that determines the stability of a colloidal dispersion is the particle size distribution. The analysis of the size distribution of encapsulated anthocyanins using zetasizer was presented in (Fig. 2). The encapsulation of anthocyanins in the CMC-PVA matrix using the ultrasonication method resulted log-normal distribution with average particle size of 304.4 nm. Therefore, encapsulated anthocyanin was categorized as nanocapsules because it had a particle size of <1000 nm[19]. The result of this study is not significantly different from the research reported by Bomba *et al.*[20]. Their work showed that encapsulation of anthocyanin-rich blueberry pomace extract using whey protein isolate (WPI) had particle sizes <400 nm. While, Garcia *et al.*[21] reported that Jaboticaba peel anthocyanin incorporated into the nanoemulsionhad particle sizes ranging 164.4-221.8 nm. This differences in particle size nano encapsulation of bioactive components are caused by several factors including the selection of stabilizers/emulsifiers/matrix, temperature and encapsulation techniques used[20-22].

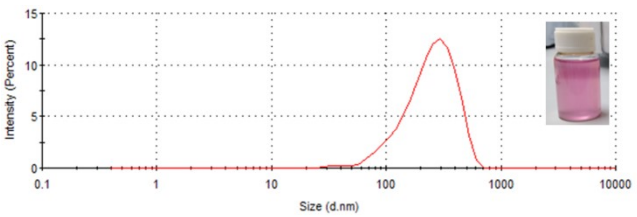

Fig. 2 — Curve of particle size distribution for encapsulated anthocyanin

In order to get the nitrite sensing results with an uniform color response which reflected a good sensitivity, encapsulated anthocyanins should be in good homogeneity. The homogeneity of the encapsulated anthocyanin distribution is exhibited by the polydispersity index (PDI), which describes the width of the particle size distribution and usually ranges from 0 to 1[23], where higher values indicate a less homogeneous particle size distribution. The polydispersity index (PDI) also provides information about the stability of the emulsion. According to Ahmed *et al.*[24] nanoemulsion is stable from the possibility of particle collision and gravity separation if the polydispersity index of 0.2 <PDI <0.6. In this work, encapsulated anthocyanins in the CMC-PVA matrix had a PDI value of 0.398, which has good homogeneity and encapsulated strongly in the CMC-PVA matrix. The comparison of PDI and the average particle size between this study and other studies is presented in (Table 2).

Thermogravimetric analysis (TGA)

Thermogravimetric analysis is used to determine the thermal decomposition process of a material through changes in its weight. CMC thermal decomposition curve showed two stages of

Table 2 — Comparison of PDI and the average particle size of encapsulated anthocyanins between this study and other studies

References	Study Results
This study	• Purple sweet potato anthocyanins • Matrix: CMC/PVA • PDI: 0.398 • Average particle size: 304.4 nm
Bamba *et al.*[20]	• Blueberry anthocyanins • Matrix: whey proteinisolate (WPI) • PDI: <0.25 • Average particle size: < 400 nm
Garcia *et al.*[21]	• Jaboticaba peel anthocyanins • Nanoemulsion system, surfactant: polysorbate 85 • PDI: 0.170–0.266 • Average particle size: 164.4–221.8 nm
Rabelo *et al.*[22]	• Juçara Palm Fruit anthocyanins • Nanoemulsion system, emulsifier: CR-310 • PDI: 0.2-0.6 • Average particle size: 146.8-814.8 nm (in the treatment)

decomposition (Fig. 3). The first stage at 38.11°C occurred an evaporation process of free and bound water of the polymer, the second stage at 275.22°C showed decomposition of the polymeric backbone in the form of saccharide ring dehydration, breaking of C-O-C bonds in the CMC chain and loss of CO_2[25]. PVA also showed the two main stages of decomposition. The first stage was at 95.42°C and the second stage was at 305.36°C. Nevertheless, at the PVA occurred a complete decomposition up to 644°C, with residues only around 3.70%. The similar result also reported by Reguieg *et al.*[26] where the maximum degradation at 372.0°C. While at CMC there was still residue as much as 37.7% since the CMC used in this study is Na-CMC (Sodium Carboxymethyl Cellulose). According to Tan *et al*.[27], Na^+ catalyses the degradation of CMC, producing the intermediate product that is most stable at high temperatures by thermal degradation in the air. In addition, Na^+ can inhibit CMC degradation to produce a relatively stable of intermediate residue.

In contrast to the CMC and PVA, CMC/PVA blend film had three stages of decomposition. The occurrence of these three stages of decomposition indicates CMC/PVA blend films have better stability[28]. The first, second, and third stages were at 48.13, 205.28, and 281.20°C, respectively. The first stage is related to dehydration, and the second stage is corresponded to the degradation of CMC/PVA[25]. CMC and PVA combination films had good stability when compared to sole CMC. However, when it was compared to CMC and PVA, the CMC/PVA curve is lower, degradation in the second stage occurs at lower temperatures. These differences may be influenced by water activity, homogeneity of chemical composition, and carbohydrate polymer of CMC in relation to degree of polymerization[29].

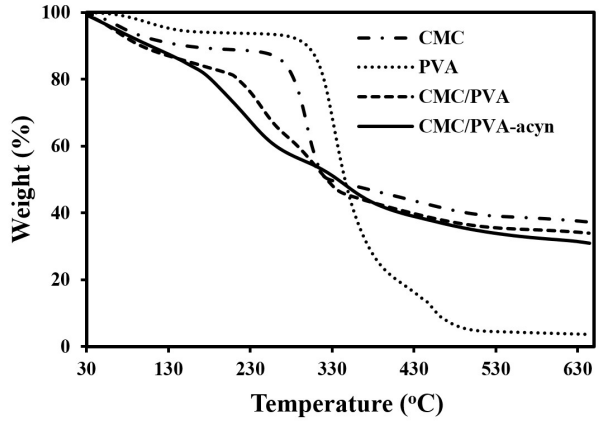

Fig. 3 — TGA termogram of CMC, PVA, CMC/PVA film and CMC/PVA-anthocyanin film

After anthocyanin incorporated into CMC/PVA film, three stages of decomposition were obtained too. The first, second, and third stages took place at 38.15, 165.33, and 313.07°C. The maximum weight loss in anthocyanin films was found at 228.99°C in the second stage of degradation. At second and third stages, anthocyanins are degraded to phenol and aldehyde by deglycosylation and ring opening reactions[30].

In this study the highest anthocyanin extract degradation occurred at 80 during 4 h of heating. In the study of Cai *et al.*[31] blueberry's anthocyanin lost the maximum weight at 130.6°C. According Mishra and Kumar[28], the high value of polymer decomposition temperature (initial temperature), final decomposition temperature, and decomposition peak temperature as well as the occurrence of three decomposition stages indicate a polymer has better stability. Therefore, the anthocyanin thermal stability increased with incorporated it into the CMC/PVA gel matrix.

Besides being thermally stable, encapsulated anthocyanins are also stable against other environmental conditions such as light and oxidation. The results of the study of Xu *et al*.[32] showed that a encapsulated anthocyanins with maltodextrin increased their stability to light after being exposed to light for 10 days. The results of Guldiken *et al*.[33] study showed that anthocyanins encapsulated with liposomes possess good physical stability for 21 storage days with the potential zeta value parameter increasing from [−25 mV] - [−28 mV] to [−26 mV - [−29 mV] and its stability against lipid oxidation also increases during 60 days of storage.

Transmission electron microscope

Transmission electron microscope is used to analyze microstructure of encapsulated anthocyanin and its interaction with nitrite. Figure 4 shows the TEM image of encapsulated anthocyanins and its interaction with nitrite. Encapsulated anthocyanin had a porous surface structure. It was gel which sphericals shape that are not bound each other and had sizes ranging from 250-400 nm (Fig. 4A). The ultrasonic homogenizer made bead anthocyanin gel well dispersed. After reacting with nitrite, encapsulated anthocyanins formed an aggregate as irregular dense spheres. Figure 4B showed the aggregation that was formed from a mixture of nitrite and encapsulated

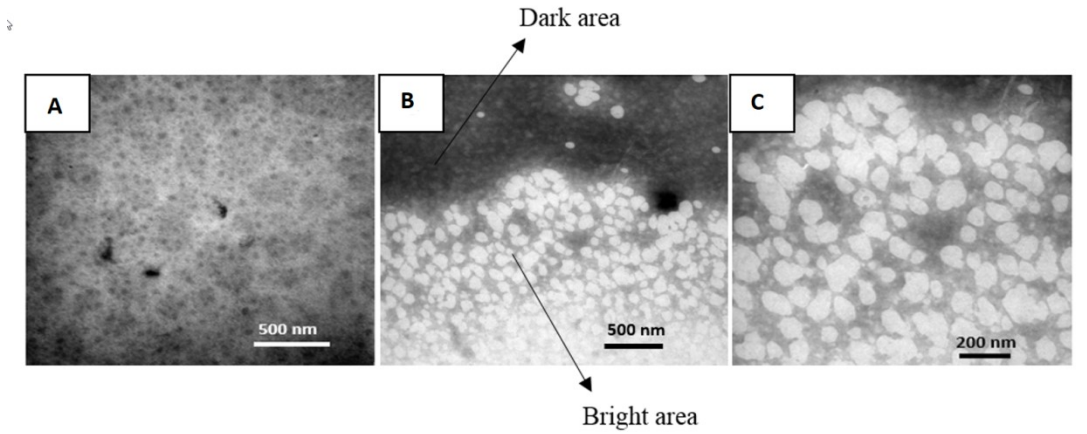

Fig. 4 — TEM image of (A) encapsulated anthocyanin; and (B & C) and aggregation of encapsulated anthocyanin-nitrite mixture

anthocyanins where the white luminescence confirmed the encapsulated anthocyanin. Figure 4C showed the irregular round crystals, which was assumed as nitrite and the area in the background as a encapsulated anthocyanin. This shows that encapsulated anthocyanins were able to react and entrap sodium nitrite without the occurrence of physical destruction. The aggregation which was form between nitrite and encapsulated anthocyanin maybe confirmed the color change of encapsulated anthocyanins from red-purple to yellow. This phenomenon was related to the research reported by Raj & Dhesingh[14].

In this study the mechanism of the aggregate formation is not through cross-linking, the aggregate is formed probably because of the transfer of electrons between the two molecules, nitrites and anthocyanins, thus forming molecules and crystals that remain intact together. According to Galán-Vidal *et al.*[34] anthocyanin color change occurs because flavylium ions on C-4 chain of anthocyanins have been substituted by nucleophilic nitrite ions. Thus, forming complex anthocyanins which cause the loss of color.

Fourier-transform infrared spectroscopy

Functional group analysis and structural description of each compound in encapsulated matrix were determined using the Fourier-Transform Infrared Spectroscopy (FTIR). Figure 5A represents the FTIR spectra of CMC/PVA film without anthocyanin. In this study the blend of CMC/PVA films showed some peaks. Sharp peak at 3294 cm^{-1} assigned as absorption band of O-H stretch vibration[35-36]. Additional peak appearance at 1724 cm^{-1} exhibited the presence of carbonyl bands from the ester

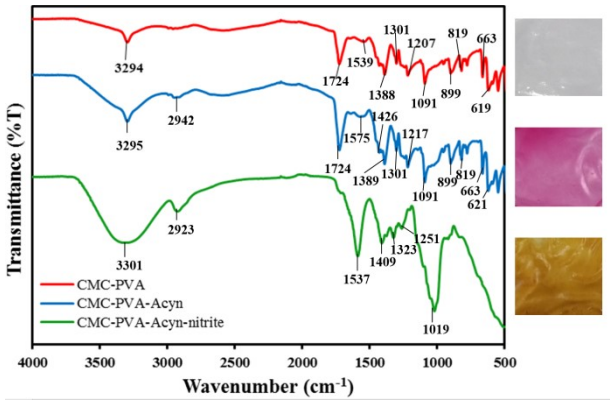

Fig. 5 — FTIR spectra of (A) CMC/PVA film; (B) CMC/PVA-anthocyanin films; and (C) CMC/PVA-anthocyanin films upon contact with nitrite

component with free carboxylic acids. Referred to Ghorpade *et al.*[37] and Mali *et al.*[25], those peaks are obtained as a result of cross-linking action of citric acid in CMC/PVA films.

FTIR spectra film of CMC/PVA- anthocyanin (CMC/PVA-acyn) was presented in (Fig. 5B). It showed that the pattern of spectra curve was similar to (Fig. 5A). There were some peak shifted and changed in peak intensity which getting stronger. Absorption peak of O-H stretch vibration shifted slightly from 3294 cm^{-1} to 3295 cm^{-1}, and the peak intensity increased sharply. Increasing of peak intensity in the O-H stretch vibration region is due to the stronger physical interactions and hydrogen bonds with polar groups between mixed polymers[38].

In this study a new peak of CMC/PVA-acyn film appeared at 2942 cm^{-1} which showed the vibration of = C-H stretch. This is due to the incorporation of anthocyanins in CMC/PVA gel matrix[39]. There was an increase in intensity at peak of 1300-1724 cm^{-1}

after anthocyanins were loaded in CMC/PVA. This proved that anthocyanins had been successfully incorporated into the polymeric of CMC/PVA matrix, because there was a modification of the type of stretching C = C from the aromatic ring.

FTIR spectra of CMC/PVA-anthocyanin reacted with nitrite was shown in (Fig. 5C). A peak of 1537 cm^{-1} appeared as symmetric N-O, indicated the presence of nitrite. As the comparison before and after interaction with nitrite, there was a shift of the O-H groups at the peak of 3295 to 3301 cm^{-1}. The region of O-H stretch became broad which indicated its damage due to increased peak at 2923 cm^{-1}. This is probably due to the formation of an anthocyanin-nitrite complex, through hydrogen bonds between molecules, which refers to Raj & Dhesingh[14]. The anthocyanin enol group on the pyran ring, at peak of 1217 cm^{-1} shifted to 1251 cm^{-1}, which can replace the C-4 ring by nitrite ions, as reported by Galán-Vidal *et al*.[34]. They described that the interaction of anthocyanins with nitrite caused anthocyanins to lose color, and maybe changed its flavylium structure become others. Its possibility was proven by the emergence of a sharp peak at 1019 cm^{-1}. The peak of 1019 cm^{-1} showed deformation of the aromatic C-H ring of anthocyanin.

Physical appearence and morfology of paper strip and its aplication for nitrite sensing

The morphology of the anthocyanin paper strip was observed by light microscope. Figure 6A shows an image of filter paper coated by anthocyanin gel bead. It formed a transparent film. Figure 6B shows a structure of paper strips, and it was clearly seen that the anthocyanin could absorb and attach into the fiber of filter paper. The anthocyanin paper strip was turned to yellow after contact with nitrites, and has a homogeneous discoloration (Fig. 6C). Nitrite solution is absorbed into the fibers of anthocyanin paper well. Therefore, the yellow color distributed homogeneously covering the paper (Fig. 6D).

Figure 7A exhibits the morphology of the Whatman No. 1 filter paper as medium of anthocyanin biosensor by SEM. It was seen that the filter paper consisted of long cellulose fibers. Anthocyanin paper strip had a very smooth and dense surface (Fig. 7B, inserted picture), and proved by SEM results in (Fig. 7B). This showed that the CMC matrix was compatible with PVA and caused simultaneously compatible with anthocyanin[10]. Therefore encapsulated anthocyanins can be homogeneous and stable coated well on the surface of the paper. Anthocyanin gel bead not only attached to the surface of the filter paper but it was well bound to the filter paper (Fig. 7B). So, when the paper was dripped with analytical chemical (nitrite), the chemical would seep slowly, without causing anthocyanin dye to release from matrix. The surface of anthocyanin paper-nitrite seemed bumpy as the forming of subtle aggregates (Fig. 7C). This was clearly seen on the cross sectionlayer where the filter paper fibers were covered by aggregates (Fig. 7D). The aggregates are formed due to the reaction of

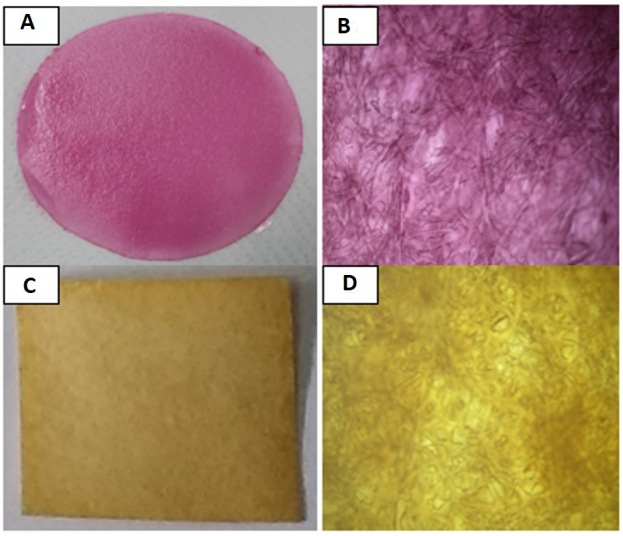

Fig. 6 — (A) Anthocyanin paper strip; (B) optical microscope image of anthocyanin paper strip; (C) Anthocyanin paper strip upon contact with nitrite; and (D) optical microscope image of anthocyanin paper strip-nitrite

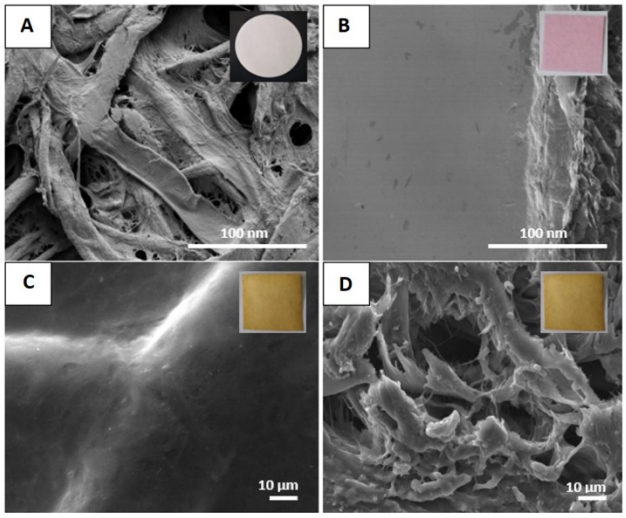

Fig. 7 — (A) SEM images of filter paper; (B) anthocyanin paper strip surface; (C) anthocyanin paper strip-nitrite surface; and (D) anthocyanin paper strip-nitrite, and cross section

nitrites with anthocyanin gel bead which may be responsible for the color changes that occured. Related to the previous research, Pourreza & Golmohammadi[40] reported about pH sensing with curcumin nanofiber, where the aggregate formed between nanocurcumin and alkaline solution confirmed the color change.

Selectivity of Anthocyanin Paper Strip and the Interferences of the Chemicals

Chemical interference with sensing nitrite by paper strip anthocyanin and its selectivity to chemicals was also observed to obtain information on its performance. Figure 8A shows that the anthocyanin paper strip is able to react with sodium nitrite. It was changing the color from red to yellow. However, no color change when it contacted with Pb^{2+}, Zn^{2+}, Fe^{3+}, Mg^{2+}, boric acid, NaCl, monosodium glutamate (MSG), sodium benzoate, and formalin (red-purple color remains). Table 3 represents the color measurements with colorimetric parameters of L^*, a^*, b^*, °Hue, and ΔE^* on anthocyanin paper strips upon contact with 10000 ppm of various chemicals.

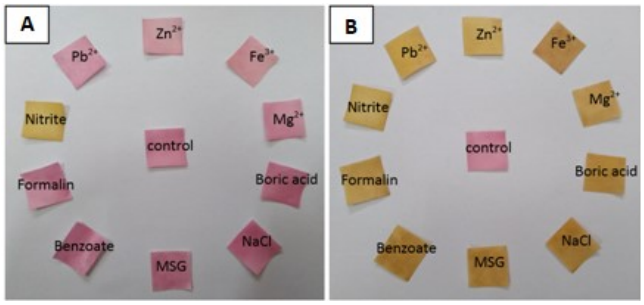

Fig. 8 — (A) Detection of anthocyanin paper strip towards 10000 ppm of various sole chemicals (a); and (B) chemicals+ nitrite mixture

Anthocyanin paper strip both before and after contacting with chemicals had L^*, a^*, b^* values in the first quadrant on CIELAB scale. All samples had L^*(lightness) values in the range of 72.44 ± 0.51 to 80.91 ± 0.29 which means bright color samples. The statistical analysis showed that L^* value in all anthocyanin strips of chemicals samples were not different significantly (P> 0.05).

The selectiveness level of anthocyanin paper strip was determined by the significantly different color parameters (a^*, b^*, c^*, °Hue and ΔE^* values) from one to other chemicals. The value of a^* on all paper strips ranged from 9.67 ± 0.30 to 25.91 ± 0.33 and b^* value was in the range -4.12 ± 0.17 to 29.92 ± 0.26. °Hue value in the paper after contact with chemicals was in the first (3.52 ± 0.40 to 72.08 ± 0.49) and the fourth (350.44 ± 0.21 to 356.77 ± 0.52) quadrants in Chroma diagram. It shows at (Table 3). All color parameters of anthocyanin paper strip-nitrite differed significantly (P< 0.05) with paper strip-other chemicals. Anthocyanin paper strip-nitrite had a °Hue value of 72.08 ± 0.49 which was classified as yellow, while the other paper strips were classified as reddish[15]. There was a significant difference color between anthocyanin paper strip (control) and anthocyanin paper strip-nitrite (P< 0.05) according to that color parameters. The results of the study from Jin& Park[41]showed that the flavonoids of *Schisandra chinensis* fruit powder in pork sausage were able to increase the red color of the meat which was marked by increasing a^* (reddish), but after nitrite was added as a preservative, the color of the sausage faded to yellow which was indicated by an increase in color b^* (yellow). It color change was an interaction between anthocyanins from *Schisandra chinensis* fruit and

Table 3 — Colorimetric characteristic of anthocyanin-paper strip against 10000 ppm of chemicals

Chemicals treatment	Color parameter					
	L^*	a^*	b^*	c^*	°Hue	ΔE^*
Control	75.48 ± 0.20^{cd}	25.91 ± 0.33^{f}	-3.73 ± 0.04^{b}	26.18 ± 0.33^{e}	351.81 ± 0.03^{d}	
Pb^{2+}	74.99 ± 0.28^{bcd}	24.43 ± 0.33^{de}	-2.17 ± 0.10^{d}	24.53 ± 0.31^{c}	354.92 ± 0.30^{f}	2.26 ± 0.28^{ab}
Zn^{2+}	78.49 ± 0.37^{e}	19.82 ± 0.48^{b}	1.17 ± 0.19^{f}	19.86 ± 0.48^{a}	3.37 ± 0.55^{a}	8.38 ± 0.18^{e}
Fe^{3+}	76.06 ± 0.60^{cd}	22.07 ± 0.78^{c}	1.36 ± 0.20^{f}	22.11 ± 0.79^{b}	3.52 ± 0.40^{a}	6.46 ± 0.46^{d}
Mg^{2+}	76.54 ± 0.29^{d}	23.28 ± 0.07^{cd}	-1.62 ± 0.01^{e}	23.34 ± 0.07^{b}	356.01 ± 0.01^{g}	3.55 ± 0.36^{bc}
Boric acid	72.44 ± 0.51^{a}	24.92 ± 0.62^{ef}	-1.4 ± 0.19^{e}	24.95 ± 0.61^{cde}	356.77 ± 0.52^{h}	4.02 ± 0.47^{c}
NaCl	72.79 ± 0.64^{a}	25.80 ± 0.89^{f}	-2.19 ± 0.03^{d}	25.89 ± 0.88^{de}	355.14 ± 0.10^{f}	3.15 ± 0.48^{abc}
MSG	76.62 ± 0.22^{d}	22.73 ± 0.21^{c}	-2.64 ± 0.02^{c}	22.88 ± 0.21^{b}	353.37 ± 0.10^{e}	3.55 ± 0.54^{bc}
Benzoate	73.74 ± 0.08^{ab}	24.54 ± 0.08^{de}	-2.9 ± 0.05^{c}	24.71 ± 0.09^{cd}	353.31 ± 0.10^{e}	2.39 ± 0.16^{ab}
Formalin	74.55 ± 1.70^{bc}	24.50 ± 0.62^{de}	-4.12 ± 0.17^{a}	24.84 ± 0.63^{cd}	350.44 ± 0.21^{c}	2.02 ± 1.16^{a}
Nitrite	80.91 ± 0.29^{f}	9.67 ± 0.30^{a}	29.92 ± 0.26^{g}	31.45 ± 0.29^{f}	72.08 ± 0.49^{b}	37.76 ± 0.08^{f}

Table 4 — Colorimetric characteristic of nitrite sensing by anthocyanin paper strip upon contact with 10000 ppm chemicals interference

Interfering chemicals	Color parameter					
	L*	a*	b*	c*	°Hue	ΔE*
Control	75.48 ± 0.20^{d}	25.91 ± 0.33^{i}	-3.73 ± 0.04^{a}	26.18 ± 0.33^{a}	351.81 ± 0.03^{g}	
Pb^{2+}	75.11 ± 0.35^{cd}	12.70 ± 0.02^{ef}	34.17 ± 0.18^{h}	36.45 ± 0.17^{h}	69.60 ± 0.13^{e}	40.13 ± 0.26^{g}
Zn^{2+}	77.12 ± 0.34^{e}	11.61 ± 0.24^{b}	31.63 ± 0.36^{g}	33.69 ± 0.42^{g}	69.85 ± 0.16^{e}	38.18 ± 0.30^{f}
Fe^{3+}	68.56 ± 0.09^{a}	15.19 ± 0.01^{h}	27.47 ± 0.03^{bc}	31.39 ± 0.03^{d}	61.07 ± 0.01^{a}	33.71 ± 0.13^{a}
Mg^{2+}	75.17 ± 0.36^{cd}	12.70 ± 0.05^{ef}	28.62 ± 0.24^{d}	31.31 ± 0.24^{d}	66.06 ± 0.11^{b}	34.94 ± 0.20^{b}
Boric acid	72.59 ± 0.32^{b}	12.92 ± 0.13^{fg}	30.66 ± 0.05^{f}	33.27 ± 0.09^{fg}	67.14 ± 0.17^{c}	36.87 ± 0.12^{e}
NaCl	74.78 ± 0.13^{c}	12.08 ± 0.06^{c}	27.87 ± 0.08^{c}	30.37 ± 0.10^{c}	66.24 ± 0.62^{b}	34.50 ± 0.20^{b}
MSG	75.04 ± 0.17^{cd}	12.49 ± 0.15^{de}	28.44 ± 0.04^{d}	31.10 ± 0.07^{d}	66.31 ± 0.31^{b}	34.86 ± 0.24^{b}
Benzoate	72.66 ± 0.16^{b}	13.16 ± 0.15^{g}	30.27 ± 0.19^{ef}	33.01 ± 0.23^{f}	66.50 ± 0.13^{b}	36.43 ± 0.17^{de}
Formalin	74.92 ± 0.06^{cd}	12.20 ± 0.11^{cd}	29.89 ± 0.25^{e}	32.28 ± 0.27^{e}	67.80 ± 0.06^{d}	36.32 ± 0.16^{d}
Nitrite	79.84 ± 0.11^{f}	9.17 ± 0.06^{a}	27.27 ± 0.10^{b}	28.77 ± 0.11^{b}	71.41 ± 0.08^{f}	35.50 ± 0.26^{c}

nitrite. Similar results were reported by Zhou *et al*.[42], wherein the addition of *Amaranthus* pigment and nitrite at a certain concentration in pork sausage led the color of the sausage to be slightly yellowish.

A ΔE^* value is responsible for the total of color difference between initial anthocyanin paper strip and anthocyanin paper strip after treatment[16]. The differences of color cannot be seen by the human eye if a value is $0.0 < \Delta E^* < 1.5$. At $1.5 < \Delta E^* < 5.0$, the color change is able seen and become clear when $\Delta E^* > 5.0$[43]. Based on that, it appeared that the color differences of the anthocyanin paper strips interact with nitrite were very clear, (thick yellow) at the ΔE^* value of 37.76 ± 0.08. Thus, anthocyanin paper strip has good selectivity for sole sodium nitrite detection.

Figure 8B shows the performance of paper strip sensor in detecting nitrite when interacted with various chemicals simultaneously (interfering chemicals). Visually, the sensing of nitrite by paper strip sensor tends had similar color (yellow color) even though it contacted with various interfering chemicals such as Pb^{2+}, Zn^{2+}, Mg^{2+}, boric acid, NaCl, monosodium glutamate (MSG), benzoate, and formalin. However, when it contacts with Fe^{3+} ion, the color shows slightly brown. According to Tai and Dempsey[44], the presence of iron is able to reduce nitrite to nitric oxide, so that iron-nitrite complexes are formed. It caused the color of anthocyanin paper strip-nitrite/Fe^{3+} changed to slightly brown colorcompared to others. However, based on b^* value, the anthocyanin paper strip-nitrite was not significantly different from the anthocyanin paper strip-nitrite/ Fe^{3+} which means they have a similar yellow color (Table 4). So that, it is assumed that anthocyanin paper strip is not interfered by the presence of Fe^{3+} when it was applied to detect nitrites in meat products. Since Fe^{3+} is available as heme iron.

Conclusion

Anthocyanin encapsulation in the CMC-PVA matrix was successfully carried out. The anthocyanin stability increased after being cooperated in the CMC-PVA matrix. Encapsulated anthocyanins have good homogeneity and encapsulated strongly in the CMC-PVA matrix. Since it had a particle size classified as nanomaterial (<1000 nm) that was 304.4 nm. Encapsulated anthocyanins had a porous surface structure and tend to form a spherical gel. As paper strip, anthocyanin gel can be coated homogeneously and stable on a paper surface with a smooth surface. It attached and it was bond well to the filter paper. So that, when it is applied to nitrite sensing, nitrite can seep slowly without causing anthocyanin dyes to release from the matrix. As a result, the interaction of nitrite and paper strips can provide a homogeneous color change response from red to yellow. Anthocyanin paper strip has good selectivity towards sodium nitrite. The results of this study provide basic information about the development of green paper strips with good stability and selectivity as a practicalsensor for nitrite detection.In the future this anthocyanin paper strip will be applied to detect nitrites in drinking water and processed meat products. This paper strip works like a litmus paper universal where color changes occur when it contacts

with the targeted chemical. It is hoped that this strips sensor can detect nitrites qualitatively and semi-quantitatively. By making a series of discolored paper strips against nitrites with various concentrations, the sensitivity range can be determined. So that the content of nitrite in drinking water and meat can be estimated by matching the color changes in the paper strip on the color series that have been made.

Conflict of interest

All authors declare no conflict of interest.

References

1 Wulandari A, Sunarti TC, Fahma F & Noor E, Potency of purple sweet potato's anthocyanin as biosensor for detection of chemicals in food products. *IOP Conf Ser: Earth Environ Sci*, 147 (2018) 1.

2 Pervaiz T, Songtao J, Faghihi F, Haider MS & Fang J, Naturally occurring anthocyanin, structure, functions and biosynthetic pathway in fruit plants. *Plant Biochem Physiol*, 5 (2017) 2.

3 Ha CT, Lien NTH, Anh ND & Lam NL, Development of natural anthocyanin dye-doped silica nanoparticles for ph and borate-sensing applications. *J Electron Mater*, 46 (2017) 6843.

4 Wu K, Zhao X, Chen M, Zhang H, Liu Z, Zhang X, Zhu X & Liu Q, Synthesis of well-dispersed Fe_3O_4 nanoparticles loaded on montmorillonite and sensitive colorimetric detection of H_2O_2 based on its peroxidase-like activity. *New J Chem*, 42 (2018) 9578.

5 Yang W, Wang J, Yang Q, Pei H, Hu N, Suo Y, Li Z, Zhang D & Wang J, Facile fabrication of robust MOF membranes on cloth via a CMC macromolecule bridge for highly efficient Pb (II) removal. *Chem Eng J*, 339 (2018) 230.

6 Kadir MFZ, Majid SR & Arof AK, Plasticized chitosan–PVA blend polymer electrolyte-based proton battery. *ElectrochimActa*, 55 (2010) 1475.

7 Saputra AH & Apriliana NH, Polyvinyl alcohol (PVA) partially hydrolyzed addition in synthesis of natural hydrogel carboxymethyl cellulose (CMC) based from water hyacinth. *MATEC Web Conf*, 156(2018) 1.

8 Winarti S, Sarofa U & Anggrahini D, Extraction and color stability of purple sweet potato (*Ipomoea batatas* L.) as natural coloring. *J Tek Kim*, 3 (2008) 207.

9 Wang BC, He R & Li ZM, The Stability and Antioxidant Activity of Anthocyanins from Blueberry. *Food Technol Biotechnol*, 48 (2010) 42.

10 Zhai X, Shi J, Zou X, Wang S, Jiang C, Zhang J, Huang X, Zhang W & Holmes M, Novel colorimetric films based on starch/polyvinyl alcohol incorporated with roselle anthocyanins for fish freshness monitoring. *Food Hydrocoll*, 69 (2017) 308.

11 Shivakumara LR, Vijayasree K, Sruthi P, Savitha KS & Demappa T, Miscibility studies of ZnO nanoparticles incorporated CMC/PVA nanocomposite films. *Indian J Adv Chem Sci*, S2 (2017) 49.

12 Anggriawan RD, Citra DA, Susiana, Putri YS, Muhamad F & Abdul RF, Performa (Paper Test Kit Formalin) as the alternative selection to improve the quality of food ingredients. *J Food Sci Qual Manag*, 31 (2014) 122.

13 Wang B, Lin Z & Wang M, Fabrication of a paper-based microfluidic device to readily determine nitrite ion concentration by simple colorimetric assay. *J Chem Educ*, 92 (2015) 733.

14 Raj S & Dhesingh RS, Curcumin based biocompatible nanofibers for lead ion detection. *Sens Actuators B*, 226 (2016) 318.

15 Kuck LS & Noreña CPZ, Microencapsulation of grape (*Vitislabrusca* var. Bordo) skin phenolic extract using gum Arabic, polydextrose, and partially hydrolyzed guar gum as encapsulating agents. *Food Chem*, 194 (2016) 569.

16 Lacerda ECQ, de Araújo CVM, Monteiro M, Finotelli PV, Torres AG & Perrone D, Starch, inulin and maltodextrin as encapsulating agents affect thequality and stability of jussara pulp microparticles. *Carbohydr Polym*, 151 (2016) 500

17 Mulyawanti I, Budijanto S & Yasni S, Stability of anthocyanin during processing, storage and simulated digestion of purple sweet potato pasta. *J Agric Sci*, 19 (2018) 1.

18 Jiang T, Mao Y, Sui L, Yang N, Li S, Zhu Z, Wang C, Yin S, He J & He Y, Degradation of anthocyanins and polymeric color formation during heat treatment of purple sweet potato extract at different pH. *Food Chem*, 274 (2019) 460.

19 Dineshkumar B, Krishnakumar K, John A, Paul D, Cherian J & Panayappan L, Nanocapsules : A Novel nano-drug delivery system. *Int J Res Drug Deliv*, 3 (2013) 1.

20 Bamba BSB, Shi J, Tranchant CC, Xue SJ, Forney CF, Lim LT, Xu W & Xu G, Coencapsulation ofpolyphenols and anthocyanins from blueberry pomace by double emulsion stabilized by whey proteins: Effect of homogenization parameters. *Molecules*, 23 (2018) 2525.

21 Garcia NOS, Fernandes CP & da Conceicao EC, Is it possible to obtain nanodispersions with jaboticaba peel's extract using low energy methods and absence of any high cost equipment?. *Food Chem*, 276 (2019) 475.

22 Rabelo CAS, Taarji N, Khalid N, Kobayashi I, Nakajima M & Neves MA, Formulation and characterization of water-in-oil nanoemulsions loaded with acai berry anthocyanins: Insights of degradation kinetics and stability evaluation of anthocyanins and nanoemulsions. *Food Res Int*, 106 (2018) 542.

23 Galindo-Rodriguez S, Allemann E, Fessi H & Doelker E, Physicochemical parameters associated with nano particle formation in the salting-out, emulsification–diffusion and nano precipitation methods. *Pharm Res*, 21 (2004) 1428.

24 Ahmed K, Yan L, David J, Clements MC & Xiao H, Nanoemulsion-and emulsion-based delivery systems for curcumin: Encapsulation and release properties. *Food Chem*, 132 (2012) 799.

25 Mali KK, Dhawele SC, Dias RJ, Dhane NS & Ghorpade VS, Citric Acid crosslinked carboxymethyl cellulose-based composite hydrogel films for drug delivery. *Indian J Pharm Sci*, 80 (2018) 657.

26 Reguieg F, Ricci L, Bouyacoub N, Belbachir M & Bertoldo M, Thermal characterization by DSC and TGA analyses of PVA hydrogels with organic and sodium MMT. *Polym Bull*, 77 (2020) 929.

27 Tan L, Shi R, Ji Q, Wang B, Quan F & Xia Y, Effect of Na^+ and Ca^{2+} on the thermal degradation of carboxymethyl cellulose in air. *Polym Polym Compos*, 25 (2017) 309.

28 Mishra V & Kumar R, Graft copolimerization of carboxymethyl cellulose: An overview. *Trends Carbohydr Res*, 4 (2012) 1.

29 Saavedra-Leos Z, Leyva-Porras C, Araujo-Díaz SB & Toxqui-Terán A, Borrás-Enríquez AJ, Technological application of maltodextrins according to the degree of polymerization. *Molecules,* 20 (2015) 21067.

30 Prietto L, Mirapalhete TC, Pinto VZ, Hoffmann JF, Vanier NL, Lim LT, Guerra Dias AR & da Rosa Zavareze E, pH-sensitive films containing anthocyanins extracted from black bean seed coat and red cabbage. *LWT - Food Sci Technol*, 80 (2017) 492.

31 Cai X, Du X, Cui D, Wang X, Yang Z & Zhu G, Improvement of stability of blueberry anthocyanins by carboxymethyl starch/xanthan gum combinations microencapsulation. *Food Hydrocoll*, 91 (2019) 238.

32 Xu Q, Li B, Wang D, Luo L, Liu G & Zhou Y, Microencapsulation and Stability Analysis of Blueberry Anthocyanins. *IOP Conf Ser Earth Environ Sci*, 252 (2019) 1.

33 Guldiken B, Gibis M, Boyacioglu D, Capanoglu E, Weiss J, Physical and chemical stability of anthocyanin-rich black carrot extract-loaded liposomes during storage. *Food Res Int*, 108 (2018) 491.

34 Galán-Vidal CA, Castañeda-Ovando A, Páez-Hernández ME & Contreras-López E, Determination of nitritees in commercial sausages by anthocyanins degradation. Experimental design and optimization. *J Mex Chem Soc*, 58 (2014) 180.

35 Yuen TA, Gopinath SCB, Anbu, P, Kasim FH, Yaakub ARW, Lakshmipriya T & Lee CG, Encapsulation of fungal extracellular enzyme cocktail in cellulose nanoparticles: enhancement in enzyme stability. *Indian J Biochem Biophys*, 56 (2019) 475.

36 Youssef AM, EL-Nagar IE, El-Torky AMM & Abd El-Hakim AA, Development and characterization of CMC/PVA films loaded with Zno-nanoparticles for antimicrobial packaging application. *Der Pharma Chem*, 9 (2017) 157.

37 Ghorpade VS, Yadav AV, Dias RJ, Mali KK, Pargaonkar SS, Shinde PV & Dhane NS, Citric acid crosslinked carboxymethylcellulose-poly (ethylene glycol) hydrogel films for delivery of poorly soluble drugs. *Int J Biol Macromol*, 118 (PtA) (2018) 783.

38 El-Hefian EA, Nasef MM & Yahaya AH, Preparation and characterization of chitosan/agar blended films: Part 1. Chemical structure and morphology. *J Chem*, 9 (2012) 1431.

39 Bulatao RM, Samin JPA, Joel R. Salazar JR & Monserate JJ, Encapsulation of anthocyanin from black rice (*Oryza sativa* L.), brand extract using chitosan-alginate nanoparticles. *J Food Res*, 6 (2017) 40.

40 Pourreza N & Golmohammadi G, Application of curcumin nanoparticles in a lab-on-paper device as a simple and green pH probe. *Talanta*, 131 (2015) 136.

41 Jin SK & Park JH, Effect of addition of *Schisandra chinensis* powder on the physico-chemical characteristics of sausage. *Asian Aust J Anim Sci*, 26 (2013) 1763

42 Zhou C, Zhang L, Wang H & Chen C, Effect of *Amaranthus* pigment on quality characteristics of pork sauage. *Asian Aust J Anim Sci*. 25 (2012):1493.

43 Óbon JM, Castellar MR, Alacid M & Fernández-López, JA, Productionof a red–purple food colorant from Opuntia stricta fruits by spray drying and itsapplication in food model systems. *J Food Eng*, 90 (2009) 471.

44 Tai YL & Dempsey BA, Nitrite reduction with hydrous ferric oxide and Fe (II): Stoichiometry, rate, and mechanism. *Water Res*, 43 (2009) 552.